Heat Capacity of Associated Systems. Experimental Data and Application of a Two-State Model to Pure Liquids and Mixtures

Claudio A. Cerdeiriña,*,† Jacobo Troncoso,† Diego González-Salgado,† Gonzalo García-Miaja,‡ Gerardo O. Hernández-Segura,‡ David Bessières,§ Milton Medeiros,‡ Luis Romaní,† and Miguel Costas*,‡

Departamento de Física Aplicada, Universidad de Vigo, Facultad de Ciencias del Campus de Ourense, 32004 Ourense, Spain, Departamento de Fisicoquímica, Facultad de Química, Universidad Nacional Autónoma de México, Cd. Universitaria, México DF 04510, México, and Laboratorie de Fluides Complexes, Groupe Haute Pression, Université de Pau et Pays de l'Adour, BP 1155, 64013 Pau, France

Received: June 27, 2006; In Final Form: October 30, 2006

The predictions from a recently reported (*J. Chem. Phys.* **2004**, *120*, 6648) two-state association model (TSAM) have been tested against experimental data. The temperature, T, and pressure, p, dependence of the isobaric heat capacity, C_p, for three pure alcohols and the temperature dependence at atmospheric pressure of the excess heat capacity, C_p^E, for four alcohol + ester mixtures have been measured. The branched alcohols were 3-pentanol, 3-methyl-3-pentanol, and 3-ethyl-3-pentanol, and the mixtures were 1-butanol and 3-methyl-3-pentanol mixed with propyl acetate and with butyl formate. These data, together with literature data for alcohol + *n*-alkane and alcohol + toluene mixtures, have been analyzed using the TSAM. The model, originally formulated for the C_p of pure liquids, has been extended here to account for the C_p^E of mixtures. To evaluate its performance, quantum mechanical ab initio calculations for the H-bond energy, which is one of the model parameters, were performed. The effect of pressure on C_p for pure liquids was elucidated, and the variety of $C_p^E(T)$ behaviors was rationalized. Furthermore, from the C_p data at various pressures, the behavior of the volume temperature derivative, $(\partial V/\partial T)_p$, was inferred, with the existence of a $(\partial V/\partial T)_p$ versus T maximum for pure associated liquids such as the branched alcohols being predicted. It is concluded that the TSAM captures the essential elements determining the behavior of the heat capacity for pure liquids and mixtures, providing insight into the macroscopic manifestation of the association phenomena occurring at the molecular level.

1. Introduction

Second-order thermodynamic quantities of pure substances, for example, C_p, $(\partial V/\partial T)_p$, and $(\partial V/\partial p)_T$, can be obtained from equations of state (EoS) by direct thermodynamic relationships. However, modeling these second derivatives of the thermodynamic potential using EoS is a difficult task, since most of them have been developed to correlate and predict fluid phase equilibria.[1−4] In general, EoS are not able to accurately reproduce phase behavior and second derivatives with a single set of adjustable parameters. As the complexity of the interactions present in the system increases, for example, when association is present, additional shortcomings appear. For instance, it is common to treat the attractive intermolecular potential with an effective function which encloses all the interactions, and hence, it is not possible to identify the various contributions to the second-order properties. An example of this situation is the VTPR group contribution EoS that has recently been shown[5] to be able to predict phase equilibria and heat capacities simultaneously, but cannot be employed to isolate the effect of association on the fluid properties. In order to gain this kind of insight and at the same time preserve reliability, more elaborated molecular based EoS must be employed, with those belonging to the SAFT[6] family being a representative example. In this context, of special relevance is the recent work of Lafitte et al.[7] and Llovell and Vega,[8] who were able to successfully describe second-order thermodynamic properties of alkanes, alkenes, and alkanols using two different versions of the SAFT. For mixtures, second-order excess properties can be modeled using either solution models as the ERAS,[9,10] SERAS,[11] UNIQUAC,[12] NRTL,[12] TK[13,14] or EoS with excess free energy mixing rules.[15,16]

The isobaric heat capacity, C_p, occupies a privileged place among the second-order properties of liquids. On one hand, due to its relation with the entropy, that is, $C_p = T(\partial S/\partial T)_p$, it provides valuable insight into the microscopic structure of the liquid, and on the other hand, it is an essential property to perform thermal calculations in all heat transfer processes. As a result, the accurate measurement and rational modeling of C_p for pure liquids and mixtures are of benefit to both the improvement of our knowledge of liquid structure and the design and optimization of many processes in the chemical industry. In particular, it has been noted that C_p is very sensitive to association phenomena, with hydrogen bonding being the most representative case.[13,14] Hence, the development of models that explicitly include association to describe C_p is important to gain insight into the basic microscopic features governing its

* Corresponding authors. Phone: (34) (988) 387217 (C.A.C.); (52) (55) 56223520 (M.C.). Fax: (34) (988) 387001 (C.A.C.); (52) (55) 56223521 (M.C.). E-mail: calvarez@uvigo.es (C.A.C.); costasmi@servidor.unam.mx (M.C.).

† Universidad de Vigo.

‡ Universidad Nacional Autónoma de México.

§ Université de Pau et Pays de l'Adour.

10.1021/jp0640272 CCC: $37.00
Published on Web 01/12/2007

experimental behavior. This has been accomplished by Llovell and Vega using the soft SAFT model[8] that provides a good description of phase equilibria and a set of properties in the Ising, mean-field, and crossover regimes. However, little attention was paid to the analysis of association effects that give rise to a remarkably rich thermodynamic behavior that, for the case of C_p, is exemplified by the different experimental temperature dependences of C_p for pure associated liquids. The rationalization in a unified description of the various $C_p(T)$ behaviors has only been reached recently using a simple two-state association model (TSAM) derived from statistical mechanical considerations.[17] The TSAM not only allowed the quantitative description of the four existing $C_p(T)$ types of curves found in the literature[18] but also predicted the existence of a fifth temperature dependence, namely, one with a maximum whose existence was corroborated experimentally with C_p measurements for highly branched alcohols. More recently, the TSAM has been successfully extended to simultaneously correlate vapor pressures and heat capacities of pure self-associated liquids.[19]

The purpose of this work is to further assess the performance of the TSAM. First, we extend our previous study on the temperature dependence of C_p to the evaluation of the effect of pressure on this property. To this end, attention is focused on the experimental determination of $C_p(T,p)$ for three pure branched alcohols of increasing sterical hindrance, where association plays a crucial role in the appearance of a $C_p(T)$ maximum at atmospheric pressure.[17] The analysis of $\partial C_p/\partial p$ using the TSAM is also relevant, since it allows the examination of the effect of association on other second-order derivatives such as the volume temperature derivative, $(\partial V/\partial T)_p$, and the volume pressure derivative, $(\partial V/\partial p)_T$. The second part of this work is devoted to the temperature dependence of the excess heat capacity, C_p^E, of associated mixtures at atmospheric pressure. We study two types of binary mixtures, namely, those containing a self-associating liquid (an alcohol) and (i) an inert (an alkane) or (ii) a noninert liquid, that is, a liquid whose molecules are proton acceptors and hence capable of forming H-bonded complexes with the self-associating liquid; here, we consider the case of a strong proton acceptor (an ester) and a weak one (an aromatic hydrocarbon). For this study, $C_p^E(T)$ values for four alcohol−ester mixtures were measured and examined together with previously reported data for alcohol−inert and alcohol−aromatic mixtures.[20,21] Since the TSAM was originally formulated for pure liquids, the analysis of the $C_p^E(T)$ data implied an extension of the model to mixtures. In addition, to evaluate the reliability of the fitted TSAM parameters, quantum mechanical ab initio calculations for the H-bond energy, which is one of the model parameters, were performed.

2. The Two-State Association Model (TSAM). Pure Liquids and Extension to Mixtures

For pure associated liquids, a detailed description of the TSAM in its original and revised versions can be found elsewhere.[17,19] Here, a description of the main results as well the extension of the model to account for both temperature and pressure dependences for pure liquids and mixtures are given. In the mean-field approximation, the isothermal−isobaric partition function, Δ, of an associated fluid, for example, a H-bonded fluid, consisting of N identical molecules is directly related to that of an individual particle, Δ_{part}, through

$$\Delta = \frac{1}{N!}(\Delta_{part})^N \tag{1}$$

where the sum over states, Δ_{part}, can be conveniently split as

$$\Delta_{part} = (\Delta_{part})_{A_i} + (\Delta_{part})_A \tag{2}$$

where $(\Delta_{part})_{A_i}$ and $(\Delta_{part})_A$ denote sums over states in which the particle is associated and dissociated, respectively. The evaluation of $(\Delta_{part})_{A_i}$ and $(\Delta_{part})_A$ is accomplished by considering two hypothetical fluids in which all molecules are associated (fluid A_i) or dissociated (fluid A). In doing so, the one-particle partition functions are expressed so as to provide a complete thermodynamic description; hence, by denoting the Gibbs energies, enthalpies, and entropies of these hypothetical fluids (in a molar basis) by G^{A_i}, G^A, H^{A_i}, H^A, S^{A_i}, and S^A, it follows that

$$(\Delta_{part})_{A_i} = \exp\left(\frac{S^{A_i}}{R} - \frac{H^{A_i}}{RT}\right) \tag{3}$$

$$(\Delta_{part})_A = \exp\left(\frac{S^A}{R} - \frac{H^A}{RT}\right) \tag{4}$$

Equation 2 can thus be rewritten as

$$\Delta_{part} = \exp\left(\frac{S^A}{R} - \frac{H^A}{RT}\right)\left[1 + \exp\left(\frac{\Delta H}{RT} - \frac{\Delta S}{R}\right)\right] \tag{5}$$

where $\Delta H = H^A - H^{A_i}$ and $\Delta S = S^A - S^{A_i}$ denote the enthalpy and entropy of dissociation. The Gibbs energy of the fluid then reads

$$G = G^A - RT\ln\left[1 + \frac{\exp(\Delta H/RT)}{r}\right] \tag{6}$$

where $r = \exp(\Delta S/R)$. Being macroscopic quantities, ΔH and ΔS (or r) depend on both T and p. To a first approximation, ΔH and ΔS can be written as

$$\Delta H = \Delta H_0 + \Delta C_p(T - T_0) + \left(\frac{\partial \Delta H}{\partial p}\right)_T (p - p_0) \tag{7}$$

$$\Delta S = \Delta S_0 + \Delta C_p \ln\left(\frac{T}{T_0}\right) + \left(\frac{\partial \Delta S}{\partial p}\right)_T (p - p_0) \quad \text{or} \tag{8}$$

$$r = r_0\left(\frac{T}{T_0}\right)^{\Delta C_p} \exp\left[\frac{(\partial \Delta S/\partial p)_T}{R}(p - p_0)\right] \tag{9}$$

where ΔH_0 and ΔS_0 denote the enthalpy and entropy of dissociation at a reference state (T_0,p_0) and $\Delta C_p = (\partial \Delta H/\partial T)_p$. From eqs 6−9, the following expression for C_p is straightforwardly derived:

$$C_p = C_p^A + R\left(\frac{\Delta H}{RT}\right)^2 \frac{r\exp(\Delta H/RT)}{[r + \exp(\Delta H/RT)]^2} - \Delta C_p \frac{\exp(\Delta H/RT)}{r + \exp(\Delta H/RT)} \tag{10}$$

In eq 10, C_p^A is the heat capacity for the hypothetical dissociated fluid, whereas the second and third terms represent the contribution to the heat capacity due to association, C_p^{assoc}, that depends on ΔH and r (or ΔS). ΔH is a measure of the strength of the interaction producing association, while ΔS is the entropy increase due to the rupture of that association and hence depends on factors such as molecular structure and density. Figure 1 shows $C_p^{assoc}(T)$ for several arbitrary sets of ΔH and r values where, for simplicity, we have taken $\Delta H =$

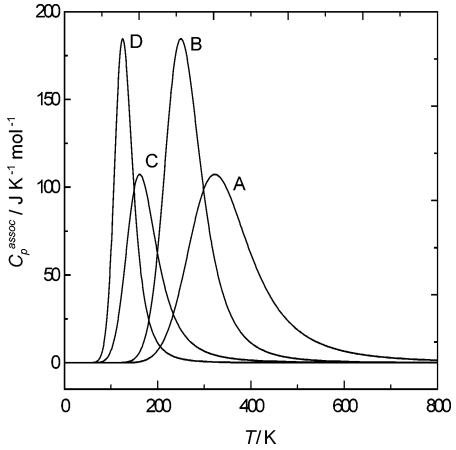

Figure 1. Associational isobaric heat capacity, C_p^{assoc}, obtained from eq 10 using the following parameter values: (A) $\Delta H_0 = 20\,000$ J mol^{-1} and $r_0 = 1000$, (B) $\Delta H_0 = 20\,000$ J mol^{-1} and $r_0 = 10\,000$, (C) $\Delta H_0 = 10\,000$ J mol^{-1} and $r_0 = 1000$, and (D) $\Delta H_0 = 10\,000$ J mol^{-1} and $r_0 = 10\,000$. For simplicity, ΔH and r were fixed to ΔH_0 and r_0 in eqs 7 and 9.

ΔH_0 and $r = r_0$, thereby neglecting their temperature and pressure dependence as given by eqs 7 and 9. It is observed that an increase of r (at constant ΔH) or a decrease of ΔH (at constant r) produces narrower peaks whose maximum is displaced toward lower temperatures. An increase of r (at constant ΔH) also results in an increase in the C_p^{assoc} values.

Finally, some comments regarding the use of eq 10 are necessary. As it is well-known, the heat capacity of a liquid can be split into two contributions, namely, the ideal gas heat capacity, C_p^{id}, and the residual heat capacity, C_p^{res}. The former is due to molecular degrees of freedom, while the latter accounts for the effect of interactions. Since the C_p^{id} values are available[22] for many pure substances, C_p^{res} can be directly evaluated from experiment and used to correlate and analyze $C_p(T)$ data. Beyond that splitting, the C_p^{res} of an associated liquid can be conveniently expressed as a sum of two contributions, namely, the association heat capacity, C_p^{assoc}, and the nonspecific heat capacity, C_p^{ns}, that is, that part of C_p^{res} which arises from interactions other than those producing association. Hence, in eq 10, $C_p^{A} = C_p^{id} + C_p^{ns}$ and the residual heat capacity is given by

$$C_p^{res} = C_p^{ns} + R\left(\frac{\Delta H}{RT}\right)^2 \frac{r\exp(\Delta H/RT)}{[r+\exp(\Delta H/RT)]^2} - \Delta C_p \frac{\exp(\Delta H/RT)}{r+\exp(\Delta H/RT)} \quad (11)$$

Extending the above-described ideas, the excess heat capacity, C_p^E, of binary mixtures containing a self-associated liquid and a nonassociated one is expressed as

$$C_p^E = (C_p^{ns})^E + (C_p^{assoc})^E = (C_p^{ns})^E + [(C_p^{assoc})^M - x(C_p^{assoc})^P] \quad (12)$$

where x denotes the mole fraction of the self-associated liquid. The two terms in eq 12 represent the nonspecific, $(C_p^{ns})^E$, and association, $(C_p^{assoc})^E$, contributions, respectively. The latter is obtained from $(C_p^{assoc})^M$ and $(C_p^{assoc})^P$, which denote the association contribution to the molar heat capacity of the mixture (M) and to the pure liquid (P), respectively. Note that, in contrast to the pure liquid case, only a fraction (the self-associated liquid mole fraction, x) of the total number of molecules are able to self-associate in the mixture. Hence,

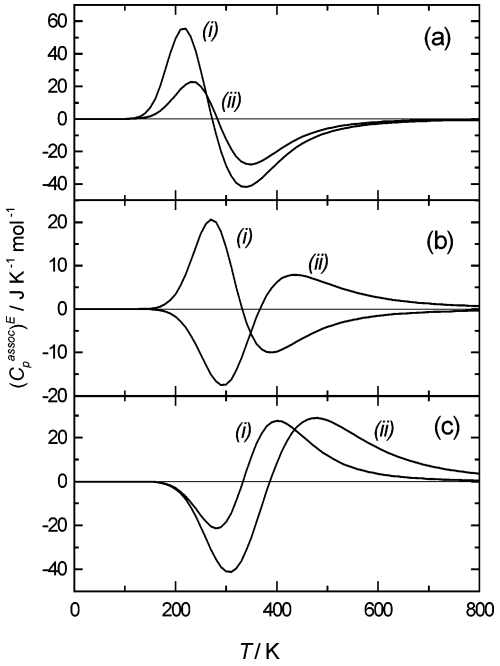

Figure 2. Associational excess isobaric heat capacity, $(C_p^{assoc})^E$, obtained from eq 15 using the following parameter values: (a) $\Delta H^M = 15\,000$ J mol^{-1}, (b) $\Delta H^M = 20\,000$ J mol^{-1}, (c) $\Delta H^M = 25\,000$ J mol^{-1}; (*i*) $r^M = 2000$, (*ii*) $r^M = 500$; $\Delta H^P = 20\,000$ J mol^{-1}, $r^P = 1000$; $\Delta C_p^P = \Delta C_p^M = 0$ in all cases.

$$(C_p^{assoc})^P = R\left(\frac{\Delta H^P}{RT}\right)^2 \frac{r^P\exp(\Delta H^P/RT)}{[r^P+\exp(\Delta H^P/RT)]^2} - \Delta C_p^P \frac{\exp(\Delta H^P/RT)}{r^P+\exp(\Delta H^P/RT)} \quad (13)$$

$$(C_p^{assoc})^M = xR\left(\frac{\Delta H^M}{RT}\right)^2 \frac{r^M\exp(\Delta H^M/RT)}{[r^M+\exp(\Delta H^M/RT)]^2} - \Delta C_p^M \frac{\exp(\Delta H^M/RT)}{r^M+\exp(\Delta H^M/RT)} \quad (14)$$

with ΔH^P, r^P, ΔH^M, and r^M given by eqs 7 and 9. Combination of eqs 12−14 gives

$$C_p^E = (C_p^{ns})^E + xR\left\{\left(\frac{\Delta H^M}{RT}\right)^2 \frac{r^M\exp(\Delta H^M/RT)}{[r^M+\exp(\Delta H^M/RT)]^2} - \Delta C_p^M \frac{\exp(\Delta H^M/RT)}{r^M+\exp(\Delta H^M/RT)} - \left(\frac{\Delta H^P}{RT}\right)^2 \frac{r^P\exp(\Delta H^P/RT)}{[r^P+\exp(\Delta H^P/RT)]^2} + \Delta C_p^P \frac{\exp(\Delta H^P/RT)}{r^P+\exp(\Delta H^P/RT)}\right\} \quad (15)$$

Figure 2 illustrates the behavior of $(C_p^{assoc})^E(T)$ for three arbitrary sets of ΔH^M and r^M, with fixed ΔH^P and r^P values (also arbitrary); again, ΔH^M, r^M, ΔH^P, and r^P were considered temperature and pressure independent. The TSAM for mixtures predicts that, depending on the ΔH^M and r^M values, the $C_p^E(T)$ behavior can change drastically from being (1) positive with a maximum at low T evolving to negative with a minimum at high T to (2) negative with a minimum at low T changing to positive with a maximum at high T. Clearly, the TSAM for mixtures can be applied to study a wide variety of mixtures

TABLE 1: Coefficients B_i of Eq 16 and Standard Deviation of Fit σ for $C_p(T, p)$ of Pure Branched Alcohols and for the Temperature Dependence of the Equimolar Excess Heat Capacity $C_p^E(T)$ of Alcohol + Proton Acceptor Mixtures

		i							
system[a]	*p*/MPa	0	1	2	3	4	5	6	σ
3P	0.1[b]	−3127.90	3432.15	−1366.235	255.567	−18.7316			0.35
	10[c]	−13.48	−397.59	390.122	−100.615	8.2031			0.13
	20[c]	178.91	−631.05	494.664	−121.202	9.7020			0.14
	30[c]	278.44	−740.87	539.175	−129.169	10.2319			0.18
	40[c]	614.14	−1128.52	705.590	−160.767	12.4693			0.18
	50[c]	701.75	−1221.12	741.666	−166.997	12.8728			0.18
	60[c]	1292.73	−1914.35	1042.353	−224.348	16.9347			0.22
3M3P	0.1[d]	29 836.38	−44 661.52	26 378.440	−7642.128	1090.3614	−61.4824		0.11
	10[e]	25 244.39	−37 782.83	22 278.716	−6426.815	911.0403	−50.9365		0.09
	20[e]	26 265.59	−39178.47	23 047.510	−6640.897	941.2077	−52.6587		0.09
	30[e]	24 206.42	−36 027.04	21 141.958	−6071.937	857.2787	−47.7636		0.10
	40[e]	19 224.50	−28 450.85	16 567.750	−4701.321	653.3738	−35.7093		0.12
	50[e]	18 861.56	−27 858.28	16 194.254	−4587.125	636.3359	−34.7125		0.12
	60[e]	24 785.44	−36 544.79	21 266.024	−6061.148	849.5545	−46.9909		0.09
3E3P	0.1[f]	112 037.74	−195 026.31	138 848.475	−51 702.709	10 638.7869	−1148.4289	50.84732	0.18
	10[g]	109 528.86	−192 505.90	138 585.414	−52 289.921	10 933.0253	−1203.5664	54.59538	0.21
	20[g]	105 804.66	−185 488.27	133 176.670	−50 105.879	10 445.0429	−1146.2677	51.82774	0.26
	30[g]	127 660.05	−222 366.17	158 968.487	−59 679.462	12 434.7665	−1365.8714	61.88644	0.29
	40[g]	125 358.54	−216 973.63	154 087.009	−57 436.404	11 875.0501	−1293.3334	58.05041	0.16
	50[g]	110 820.02	−191 574.91	135 719.567	−50 399.302	10 368.3430	−1122.3497	50.01274	0.30
	60[g]	139 623.08	−241 431.06	171 611.798	−64 158.162	13 330.5319	−1461.9354	66.20593	0.15
1-butanol + PA	0.1[h]	512.98	−722.49	380.211	−86.757	7.1824			0.02
1-butanol + BF	0.1[h]	646.92	−921.02	485.756	−110.533	9.1223			0.02
3M3P + PA	0.1[h]	−7145.29	9305.40	−4482.660	947.758	−74.3869			0.03
3M3P + BF	0.1[h]	−8140.40	10 512.150	−5024.932	1055.606	−82.4403			0.04

[a] 3P, 3M3P, and 3E3P stand for 3-pentanol, 3-methyl-3-pentanol, and 3-ethyl-3-pentanol, respectively. PA and BF stand for propyl acetate and butyl formate, respectively. [b] From 278.15 to 378.15 K. [c] From 278.15 to 421.15 K. [d] From 278.15 to 381.15 K. [e] From 278.15 to 403.15 K. [f] From 278.15 to 401.15 K. [g] From 278.15 to 420.15 K. [h] From 278.15 to 338.15 K.

even if the available experimental window only allows the measurement of a portion of the $C_p^E(T)$ curve.

3. Methods

3.1. Materials. All chemicals were from Aldrich with a purity greater than 98% for 3-ethyl-3-pentanol (3E3P), 99% for 3-methyl-3-pentanol (3M3P), 99.5% for 3-pentanol (3P), 99.5% for 1-butanol, 99% for propyl acetate (PA), and 99% for butyl formate (BF). Prior to use, they were dried over 0.4 nm molecular sieves and degassed.

3.2. Experimental Procedures. Heat capacity measurements were performed using two different calorimeters, the Setaram C-80 (Pau laboratory) and the Setaram Micro DSC II (Ourense laboratory). Since both pieces of equipment determine the volumetric heat capacity, the obtention of molar heat capacities, C_p, entails density, ρ, measurements. In both laboratories, ρ was determined using an Anton-Paar 512P vibrating tube densimeter described elsewhere.[23,24] Detailed information about the C-80 and the Micro DSC II, including calibration procedures and pressure implementation, can be found in refs 25 and 26, respectively. Both calorimeters operate under the same principle, that is, Calvet calorimetry with temperature control. Here, the scanning method was used; that is, a temperature variation at a constant rate (0.15 K min^{-1}) was induced under isobaric conditions and the calorimetric response was recorded. Calibrations were made using heat capacity standards. Two main differences between the C-80 and the Micro DSC must be mentioned, namely, the operating ranges and the quality of measurements. The C-80 allows one to obtain data up to 100 MPa and within the temperature interval 303.15−423.15 K, while the Micro DSC II operates over narrower ranges (up to 60 MPa and from 273.15 to 363.15 K). The estimated uncertainty on C_p, based mainly on the estimated errors due to calibration, is approximately 0.2% in both cases; however, the reproducibility of the measurements is better for the Micro DSC II.

The $C_p(T,p)$ values of the three pure branched alcohols, namely, 3-pentanol, 3-methyl-3-pentanol, and 3-ethyl-3-pentanol, were determined using both calorimeters. Table 1 contains all the information about the working (T,p) ranges. For each alcohol at each pressure, data were measured from 278.15 to 338.15 K using the Micro DSC II and from 313.15 K on using the C-80. They were carefully examined with particular emphasis on the overlapping temperature interval, where very good agreement (within the experimental uncertainties) was found. Also, data at atmospheric pressure were found to be in good agreement with previously reported values.[17,27] The four binary mixtures studied were equimolar samples containing (1-butanol or 3-methyl-3-pentanol) and (propyl acetate or butyl formate), with their excess heat capacities, C_p^E, being measured using the Micro DSC II at atmospheric pressure in the 278.15−338.15 K temperature range. All of the data measured in this work can be found as Supporting Information.

The $C_p(T)$ values for each alcohol at each pressure and $C_p^E(T)$ values for each mixture were fitted to a polynomial of the form

$$Y = \sum_{i=0}^{n} B_i \left(\frac{T}{100}\right)^i \tag{16}$$

where Y can be C_p or C_p^E. Fits were performed using the software Origin 7.0, with the final values of the coefficients B_i together with the standard deviations being listed in Table 1.

3.3. Quantum Mechanical Calculation of H-Bond Energies. Hydrogen bond energies, $\Delta\epsilon$, between the hydrogen in the hydroxyl group of an alcohol and (i) each of the oxygen atoms in an ester and (ii) the aromatic ring of toluene have been

estimated using quantum mechanics MP2 ab initio calculations performed with the Gaussian 94 program[28] and the 6-31G* basis set.[29] Calculations were done for methanol, 1-butanol, butyl formate, and toluene monomers, and the following three dimers: methanol/toluene, 1-butanol/butyl formate (ester oxygen), and 1-butanol/butyl formate (carbonyl oxygen). The monomer energy, ϵ_A, was obtained in the optimized geometry from the appropriate initial configurations: for methanol, the dihedral $H_1-O_2-C_3-H_4$ was set to 180°, for 1-butanol, the all-trans configuration with all dihedral angles was set to 180°, for toluene, all carbon atoms were in the same plane, and for butyl formate ($C_1-C_2-C_3-C_4-O_5-C_6-O_7$), the dihedral angles were selected to 180° for $C_1-C_2-C_3-C_4$, $C_2-C_3-C_4-O_5$, and $C_3-C_4-O_5-C_6$ and to 0° for $C_4-O_5-C_6-O_7$. The dimer energies, ϵ_{AB}, were calculated in the optimized geometry obtained from the initial configurations in which two monomers A and B (in their optimized geometry) were placed in such a way that the distance between the proton acceptor or the aromatic ring and hydrogen in the hydroxyl group was typical of H-bond distance and the repulsion between all the atoms is small. In all of the cases, the local minimum character was ensured using the harmonic vibration frequencies calculation. The optimized geometries for monomers and dimers are reported as Supporting Information. The H-bond energy, $\Delta\epsilon$, was finally determined as the difference between the monomer energy, $\epsilon_A + \epsilon_B$, and the dimer energy, ϵ_{AB}, corrected by the basis set superposition error (BSSE).[30] The obtained $\Delta\epsilon$ values (in J mol^{-1}) were 10 565 for methanol/toluene, 10 695 for 1-butanol/butyl formate (ester oxygen), and 16 110 for 1-butanol/butyl formate (carbonyl oxygen). These values contrast with those for a H-bond between two hydroxyl groups in linear alcohols (from methanol to 1-pentanol, an average $\Delta\epsilon$ value of 21 182 J mol^{-1}) reported in ref 17.

4. Results and Discussion

4.1. Temperature and Pressure Dependence of the Heat Capacity of Pure Branched Alcohols. The experimental $C_p(T,p)$ values for 3-pentanol (3P), 3-methyl-3-pentanol (3M3P), and 3-ethyl-3-pentanol (3E3P) are displayed in Figure 3 at atmospheric pressure and 60 MPa, the highest pressure employed here. For 3M3P and 3E3P, $C_p(T)$ displays a maximum at all pressures. For 3P, the maximum is not seen at atmospheric pressure but an increase of pressure, that is, widening of the temperature interval where 3P is a liquid, allowed the detection of the maximum starting at 10 MPa. For a given alcohol, the temperature where C_p is maximum is practically the same within the employed 0.1−60 MPa pressure range. The effect of pressure is basically to reduce the magnitude of $C_p(T)$ by a small amount, without significantly changing its temperature dependence. The comparison between the three alcohols shows that, in going from 3P to 3E3P, the $C_p(T)$ maximum is significantly displaced toward lower temperatures.

The application of the TSAM consisted of fitting the $C_p^{res}(T,p)$ data employing eq 11 with ΔH and r given by eqs 7 and 9, respectively; C_p^{res} values were obtained using the C_p^{id} values given in ref 22 for 3P and 3M3P, whereas the Benson group contribution method[31] was used for obtaining the C_p^{id} values of 3E3P. Previous applications of the model showed that, to a good approximation, ΔH and r can be regarded as temperature independent.[17,19] Indeed, the $\Delta H(T)$ values for methanol obtained from Monte Carlo simulations[19,32] support the assumption $\Delta C_p \approx 0$. In addition, preliminary fits to the data showed that $(\partial\Delta S/\partial p)_T \approx 0$. Regarding C_p^{ns}, which was considered constant in previous works,[17,19] here, we have taken into account its temperature and pressure dependence. Thus, to a first approximation,

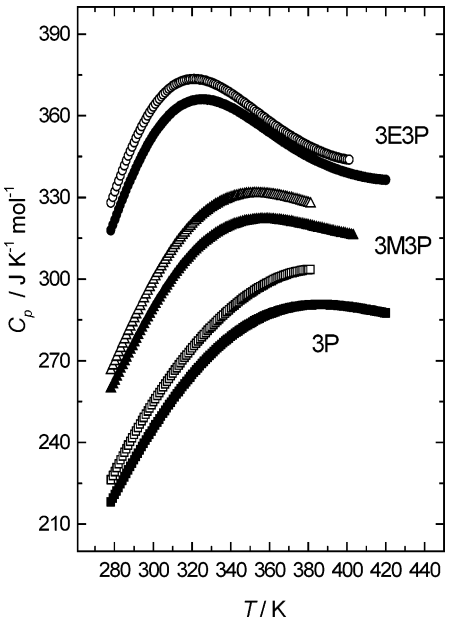

Figure 3. Experimental isobaric heat capacities, $C_p(T,p)$, for 3-pentanol (3P), 3-methyl-3-pentanol (3M3P), and 3-ethyl-3-pentanol (3E3P) at 0.1 MPa (open symbols) and at 60 MPa (closed symbols). $C_p(T,p)$ data can be found as Supporting Information. The data shown are from the smoothing eq 16 with the parameters in Table 1.

$$C_p^{ns} = (C_p^{ns})_0 + (\partial C_p^{ns}/\partial T)_p(T - T_0) + (\partial C_p^{ns}/\partial p)_T(p - p_0) \quad (17)$$

The fitting approach outlined above produced a set of parameters [ΔH_0, $(\partial\Delta H/\partial p)_T$, r, $(C_p^{ns})_0$, $(\partial C_p^{ns}/\partial T)_p$, and $(\partial C_p^{ns}/\partial p)_T$] for each alcohol, with their values being reported in Table 2. The reference temperature, T_0, and pressure, p_0, were fixed to 298.15 K and 0.1 MPa, respectively. The parameter values for 3M3P and 3E3P differ slightly from those in ref 17, since, here, data in a wider temperature interval have been used and they were treated according to a different fitting approach. The good performance of the model is shown in Figure 4 for the data at 20 and 50 MPa, with the fittings at all the other pressures being of similar quality. Table 2 shows that the ΔH values are essentially the same for the three alcohols. Their average value is 20 124 J mol^{-1}, close to previously reported ΔH values for many linear and branched alcohols as well as with quantum mechanical calculations of the H-bond energy between hydroxyl groups (see section 3.3) The r values, a measure of the dissociation entropy, ΔS, are markedly different for the three alcohols. In particular, r increases in going from 3P to 3E3P, that is, with an increase of steric hindrance over the hydroxyl group of the alcohol. This result is reasonable, since the entropy change caused by the disruption of H-bonds must increase with an increase of steric hindrance. The r values in Table 2 are 1.3, 2.6, and 5.0 times bigger than those for the corresponding isomeric 1-alcohols in ref 17 where no C_p maximum is observed at atmospheric pressure. The C_p maximum arises when a sharp C_p^{assoc} peak (large r value) compensates the positively sloped C_p^{id}, with these conditions being fulfilled by the branched alcohols. Figure 1 indicates that, as the r value increases, the sharper the peak becomes and the lower the temperature where its maximum occurs. Thus, the appearance of the maximum as well as its displacement toward lower temperatures in going from 3P to 3E3P are explained by the model.

TABLE 2: TSAM Parameters for Pure Branched Alcohols[a]

ΔH_0 (J mol^{-1})	$(\partial\Delta H/\partial p)_T$[b] (J MPa^{-1} mol^{-1})	r	$(C_p^{ns})_0$ (J K^{-1} mol^{-1})	$(\partial C_p^{ns}/\partial T)_p$ (J K^{-2} mol^{-1})	$(\partial C_p^{ns}/\partial p)_T$[c] (J K^{-1} MPa^{-1} mol^{-1})	χ^2
			3P			
19579 ± 201	−1.61 ± 0.16	430 ± 26	58.02 ± 0.54	0.073 ± 0.004	−0.170 ± 0.001 [−0.15]	0.58
			3M3P			
19910 ± 40	0.06 ± 0.09	814 ± 10	49.46 ± 0.18	0.119 ± 0.013	−0.160 ± 0.001 [−0.16]	0.30
			3E3P			
20884 ± 22	3.85 ± 0.1	2113 ± 18	49.17 ± 0.07	0.181 ± 0.001	−0.133 ± 0.001 [−0.12]	0.47

[a] Fitted using eq 11 with ΔH, r, and C_p^{ns} given by eqs 7, 9, and 17, respectively; $\Delta C_p = (\partial\Delta S/\partial p)_T = 0$, $T_0 = 298.15$ K, and $p_0 = 0.1$ MPa in eqs 7 and 9. C_p^{res} was calculated every degree using eq 16 (see text). The temperature intervals used in the fitting process are indicated in Table 1. 3P, 3M3P, and 3E3P stand for 3-pentanol, 3-methyl-3-pentanol, and 3-ethyl-3-pentanol, respectively. [b] $(\partial\Delta H/\partial p)_T = \Delta V$. [c] Values in brackets are the experimental $(\partial C_p/\partial p)_T$ values at the temperature of the C_p maximum.

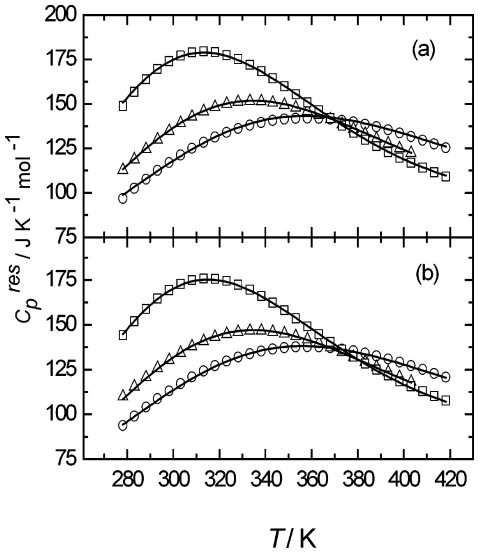

Figure 4. Residual heat capacities, C_p^{res}, for 3-pentanol (○), 3-methyl-3-pentanol (△), and 3-ethyl-3-pentanol (□) at 20 MPa (a) and at 50 MPa (b). Curves are C_p^{res} from eq 11 using the parameter values in Table 2. Although the fittings to C_p^{res} were performed using data every degree, here, for clarity, data are shown every 5°.

It is also interesting to examine the effect of pressure on C_p. Table 2 indicates that $(\partial C_p^{ns}/\partial p)_T$ is negative, in agreement with the above-noted fact that the effect of pressure is to decrease, albeit by a small amount, the magnitude of C_p. Calculations using Flory theory[33] showed that the residual heat capacities of *n*-alkanes decrease with increasing pressure. The fact that the $C_p^{ns}(p)$ behavior found here is qualitatively the same as that produced by a successful theory for nonassociating liquids such as Flory theory points toward the reliability of the TSAM. At this point, it is worth mentioning that, at the temperature where the C_p^{assoc} maximum occurs (which practically coincides with that of the C_p maximum), the model predicts that $(\partial C_p/\partial p)_T = (\partial C_p^{ns}/\partial T)_T$. The very good agreement between the experimental $(\partial C_p/\partial p)_T$ and the fitted $(\partial C_p^{ns}/\partial T)_T$ values shown in Table 2 supports this prediction and reflects the goodness of the fitting approach. The comparison between the $(\partial C_p^{ns}/\partial p)_T$ values in Table 2 and the directly evaluated $(\partial C_p/\partial p)_T$ values from the experimental data indicates that the association contribution to $(\partial C_p/\partial p)_T$ is significantly less important than the nonspecific one, with the relative weight of the latter being as much as 80%. In contrast, it is found that $\partial C_p/\partial T$ is mainly governed by the association contribution, with the relative weight of the nonspecific contribution being less than 30%. Accounting for only 20% of the total $\partial C_p/\partial p$, it is reasonable to expect that the effect of association on $\partial C_p/\partial p$ must be difficult to detect. However, careful inspection of the $C_p(T,p)$ data for 3E3P (Figure 3) shows that, in the temperature range above the maximum, $\partial C_p/\partial p$ decreases with T, becoming very small at high temperatures. On the basis that C_p^{ns} varies with T and p as indicated by eq 17, this experimental behavior must reasonably be regarded as an association effect. Given the exact thermodynamic relation $(\partial C_p/\partial p)_T = -T(\partial^2 V/\partial T^2)_p$, it is useful and instructive to alternatively rationalize the effect of pressure on C_p by examining the behavior of the volume temperature derivative, $(\partial V/\partial T)_p$, in the framework of the TSAM. Taking into account that we have assumed $(\partial\Delta S/\partial p)_T = 0$, differentiation of eq 6 leads to the following expression for $(\partial V/\partial T)_p$:

$$\left(\frac{\partial V}{\partial T}\right)_P = \left(\frac{\partial V}{\partial T}\right)_P^A + \frac{\Delta H \Delta V}{RT^2}\frac{r\exp(\Delta H/RT)}{[r+\exp(\Delta H/RT)]^2} \qquad (18)$$

where $\Delta V = V^A - V^{A_i} = (\partial\Delta H/\partial p)_T$ is the volume change upon dissociation. Since $(\partial\Delta H/\partial p)_T$ is constant, ΔV is both temperature and pressure independent. Note that the second term in the right-hand side of eq 18, that is, the associational contribution, $(\partial V/\partial T)_p^{assoc}$, has the same temperature dependence as C_p^{assoc} (assuming that $\Delta C_p = 0$ in eqs 10 and 11), with the only difference being the multiplying factor ($\Delta H\Delta V$ for $(\partial V/\partial T)_p^{assoc}$ and ΔH^2 for C_p^{assoc}). In other words, the $(\partial V/\partial T)_p^{assoc}$ versus T curves are qualitatively the same as those for C_p^{assoc} in Figure 1. Using the ΔV values in Table 2, $(\partial V/\partial T)_p^{assoc}$ can be estimated, with the resulting values for 3E3P being displayed in Figure 5a where for comparison the calculated values for its linear alcohol isomer (1-heptanol) are also shown ($\Delta V = 5$ cm^3 mol^{-1} from ref 34). As expected, the effect of association is larger for 3E3P than for 1-heptanol due to its bigger r value. In particular, the predicted $(\partial V/\partial T)_p^{assoc}$ value for 3E3P passes through a maximum, while that for 1-heptanol increases monotonically with T. Hence, according to eq 18, the curvature of $(\partial V/\partial T)_p$ for these two isomeric alcohols must be quite different, as in fact is corroborated by the experimental data shown in Figure 5b. Note that no model values are shown in Figure 5b, since the nonspecific contribution, $(\partial V/\partial T)_p^A$, in eq 18 is difficult to characterize. As T increases, the experimental $(\partial V/\partial T)_p$ versus T curve for 3E3P appears to be going toward a maximum, with this behavior being consistent with the small $(\partial C_p/\partial p)_T$ value seen in Figure 3. These results noticeably indicate that, although in a smoother way (owing to the smallness of ΔV), the temperature dependence of $(\partial V/\partial T)_p$ for pure associated liquids is subjected to similar effects as those observed for C_p. In

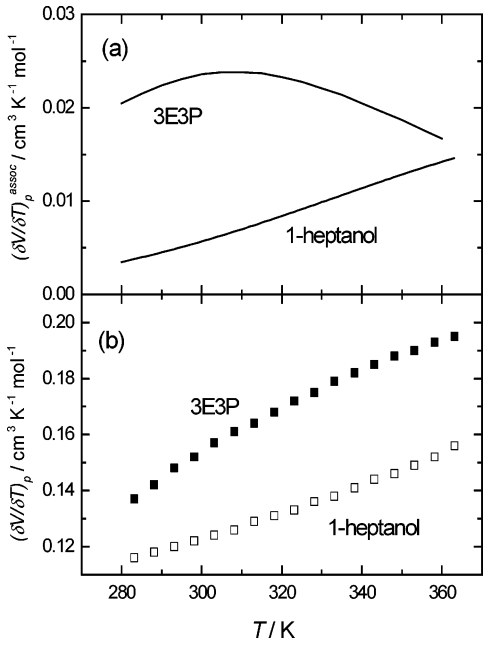

Figure 5. (a) Associational volume temperature derivative, $(\partial V/\partial T)_p^{assoc}$, for 3-ethyl-3-pentanol (3E3P) and for 1-heptanol calculated from eq 18 and (b) experimental volume temperature derivative, $(\partial V/\partial T)_p$, for 3E3P from ref 35 and for 1-heptanol from ref 36.

particular, it is predicted that as a consequence of association effects $(\partial V/\partial T)_p$ must display a maximum for branched alcohols. Clearly, 3E3P is a good candidate to corroborate this prediction and hence measuring $(\partial V/\partial T)_p$ for this alcohol above 360 K is an attractive option for future experimental work. In this context, it is worthwhile to question what the effect of association on the volume pressure derivative, $(\partial V/\partial p)_T$, is. Within the TSAM, differentiation of eq 6 gives

$$-\left(\frac{\partial V}{\partial p}\right)_T = -\left(\frac{\partial V}{\partial p}\right)_T^{A} + \frac{\Delta V^2}{RT}\frac{r\exp(\Delta H/RT)}{[r+\exp(\Delta H/RT)]^2} \qquad (19)$$

where the second term is $(\partial V/\partial p)_T^{assoc}$. Equation 19 indicates that the effect of association on $(\partial V/\partial p)_T$ is negligible owing to the small value of the multiplying factor ΔV^2.

Finally, it is interesting to discuss the ΔV values in Table 2. ΔV is seen to increase from negative to positive values as the steric hindrance over the hydroxyl group of the alcohol increases in going from 3P to 3E3P. Although negative ΔV seems to be physically unreasonable, there are systems showing such behavior, with pure water being the most representative case.[37] From the molecular structure of 3P, it appears possible that the net volume occupied by two neighboring monomers that have their hydrocarbon chains aligned and their hydroxyl groups pointing toward opposite directions is smaller than the net volume of an associated dimer where, necessarily, the hydroxyl groups of each molecule are joined by a H-bond and their chains are far apart. Hence, such geometrical arrangements for adjacent monomers and for a H-bonded dimer could produce $\Delta V < 0$. In contrast, due to their branched hydrocarbon chains, nonassociated monomers of 3M3P and 3E3P cannot form such a "packed" geometry. Elucidating whether the unexpected negative ΔV value for 3P is a fitting artifact or it represents a real physical behavior deserves further study.

4.2. Excess Heat Capacities. *4.2.1. Alcohol + Inert Mixtures.* For alcohol + inert mixtures, the self-association capability of alcohol molecules is lower than that in the pure alcohol. The formation of hydrogen bonds in solution corresponds to bringing

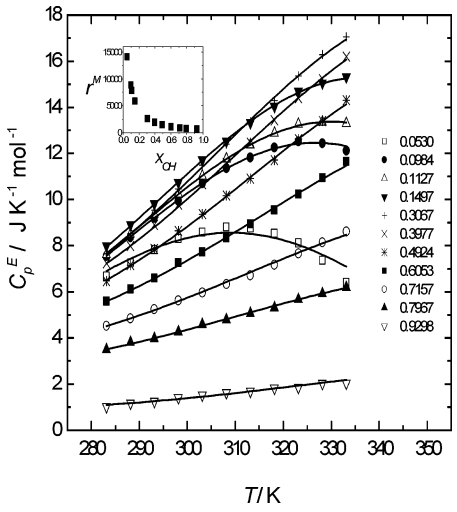

Figure 6. Excess heat capacities, C_p^E, for 1-decanol + *n*-decane at the indicated alcohol mole fractions. Data are from ref 21. Curves are C_p^E from eq 15 using the parameter values in Table 3. Although the fittings to C_p^E were performed using data every degree, here, for clarity, data are shown every 5°. The inset shows r^M against alcohol mole fraction (see text).

together alcohol molecules over longer distances than in the pure alcohol. In other words, the dissociation entropy must increase upon mixing, that is, $r^M > r^P$. On the basis that $\Delta H^M = \Delta H^P$, which can be regarded as a good approximation, the qualitative $C_p^E(T)$ behavior predicted by the TSAM is that depicted in Figure 2b-(*i*).

The experimental $C_p^E(T)$ data for 1-decanol + *n*-decane (*n*-C_{10}) at 11 concentrations[21] and for 1-butanol and 3M3P + *n*-C_{10} at 3 concentrations[20] (low, equimolar, and high alcohol mole fraction) are shown in Figures 6 and 7, respectively. It is seen that, in the same temperature interval, different regions of the "master" C_p^E versus T curve (Figure 2b-(*i*)) are observed. This finding has been previously rationalized qualitatively using the same basic concepts employed to develop the TSAM.[20] Here, we quantitatively apply the extension of the TSAM to mixtures given by eq 15. In doing so, the pure alcohol parameters ΔH^P and r^P were kept fixed and equal to those given in ref 17 for 1-butanol and 1-decanol and in Table 2 (at atmospheric pressure) for 3M3P, leaving ΔH^M, r^M, and $(C_p^{ns})^E$ as adjustable parameters. Implicit in this fitting strategy is that ΔC_p is, as in the pure liquid case, set to zero. Also, $(C_p^{ns})^E$ has been considered as temperature independent, an assumption which is better fulfilled the narrower the working temperature interval is; the fact that the present data cover 60° justifies this approximation. For simplicity, a parabolic dependence for $(C_p^{ns})^E$ with alcohol mole fraction was assumed, that is, $(C_p^{ns})^E = Dx_{OH}(1 - x_{OH})$, with D being a constant. The resulting values for the parameters are given in Table 3, with the quality of the fittings being displayed in Figures 6 and 7. Clearly, the TSAM extension to mixtures is able to capture the essential elements determining the $C_p^E(T)$ behavior for these alcohol + inert mixtures.

In Table 3, the ΔH^M values needed to adequately fit the data are slightly different from those for the corresponding pure alcohols. This may not be surprising, since a change in the environment of a given molecule upon mixing must affect its energy to a certain extent. On the other hand, the r^M values in Table 3 and the inset of Figure 6 (for 1-decanol + *n*-C_{10}) are seen to significantly increase with decreasing alcohol concentration, with this dependence being well represented by a power law, $r^M = r^P(x_{OH})^k$. In the alcohol diluted region, this increase

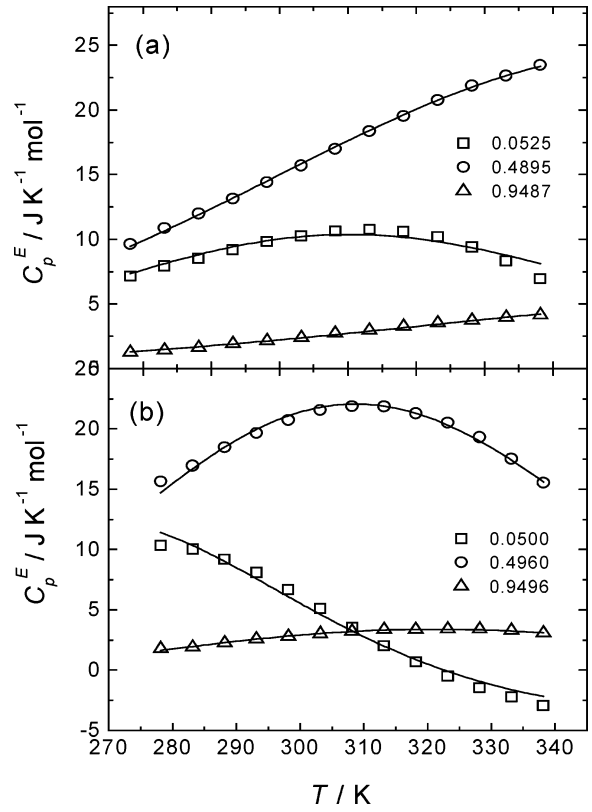

Figure 7. Excess heat capacities, C_p^E, for 1-butanol + *n*-decane (a) and 3M3P + *n*-decane (b) at the indicated alcohol mole fractions. Data are from ref 20. Curves are C_p^E from eq 15 using the parameter values in Table 3. Although the fittings to C_p^E were performed using data every degree, here, for clarity, data are shown at less temperatures.

TABLE 3: TSAM Parameters for Alcohol + Inert Mixtures[a]

x_{OH}	ΔH^M (J mol^{-1})	r^M
	1-Decanol + *n*-Decane[b]	
0.053	26272 ± 35	14114 ± 157
0.0984	26732 ± 32	8857 ± 87
0.1127	26744 ± 32	7854 ± 74
0.1497	26554 ± 31	5877 ± 51
0.3067	25793 ± 33	2632 ± 21
0.3977	25346 ± 34	1926 ± 15
0.4924	24846 ± 33	1443 ± 11
0.6053	24262 ± 29	1084 ± 7
0.7157	23730 ± 24	856 ± 5
0.7967	23456 ± 20	755 ± 4
0.9298	23323 ± 16	678 ± 3
	1-Butanol + *n*-Decane[c]	
0.0525	27228 ± 169	23444 ± 1567
0.48952	22990 ± 165	783 ± 20
0.9487	23213 ± 125	311 ± 10
	3M3P + *n*-Decane[d]	
0.05	28467 ± 217	234203 ± 26411
0.4959	23201 ± 100	4116 ± 182
0.9487	20267 ± 21	953 ± 6

[a] Fitted using eq 15 using the procedure described in the text. The temperature interval used in the fitting process (C_p^E every degree from refs 20 and 21) was 283.15−333.15 K for 1-decanol + *n*-decane and 278.15−338.15 K for 1-butanol + *n*-decane and 3M3P + *n*-decane. 3M3P stands for 3-methyl-3-pentanol. [b] ΔH^P = 23124 J mol^{-1}. r^P = 627.4. D = 12.6 ± 0.3 J K^{-1} mol^{-1}. χ^2 = 0.0091. [c] ΔH^P = 23124 J mol^{-1}. r^P = 264.4. D = 0.74 ± 2 J K^{-1} mol^{-1}. χ^2 = 0.0606. [d] ΔH^P = 19910 J mol^{-1}. r^P = 814. D = −18.7 ± 2.5 J K^{-1} mol^{-1}. χ^2 = 0.12216.

becomes dramatic. Then, the TSAM predicts a large entropic effect due to the formation of H-bonded species at low alcohol concentrations, which is consistent with the fact that the formation of hydrogen bonds in solution corresponds to bringing together alcohol molecules over very long distances. In summary, both ΔH^M and r^M depend on x_{OH}; however, the former is significantly less sensitive to changes in composition. Table 3 also indicates that the D values change sign from mixture to mixture. This behavior is difficult to rationalize on physical terms, and it is seen as a consequence of the simplicity of both the TSAM and the employed functional form for the nonspecific contribution, $(C_p^{ns})^E$. In fact, it has been observed that the TSAM is unable to fit satisfactorily $C_p^E(T)$ data at very low alcohol concentrations ($x_{OH} < 0.05$) where there might be other effects, for example, hydrogen bond cooperativity,[38] that escape the TSAM basic and simple considerations. Introducing these effects is clearly an avenue for future improvement.

4.2.2. Alcohol + Noninert Mixtures. When the inert liquid is substituted by a proton acceptor compound, that is, a substance that while unable to self-associate is however capable of forming H-bonded species with the alcohol molecules, the $C_p^E(T)$ reflects a competition between the two associating processes, namely, the alcohol self-association and the alcohol−proton acceptor complex formation.[39] In principle, in order to quantitatively describe this situation, it would be necessary to distinguish between self-associated species and alcohol−proton acceptor complexes. This could be accomplished (see eq 1 and subsequent derivations) by splitting the one-particle partition function, Δ_{part}, into three parts, namely, $(\Delta_{part})_A$, $(\Delta_{part})_{A_i}$, and $(\Delta_{part})_{AB}$, with the latter two corresponding to states where the alcohol molecule is self-associated or is forming a complex with a molecule, B, of the proton acceptor, respectively. Then, a new hypothetical fluid, AB, that is, that consisting of alcohol molecules forming cross complexes, would have to be considered, thereby introducing two new parameters, namely, the enthalpy and entropy difference between the dissociated and "complex" hypothetical fluids. When applying such a "three-state model" to the data, too many adjustable parameters (five) would be necessary. Given this situation, we used the TSAM extension to mixtures described in section 2. In doing so, we are considering only two hypothetical fluids (fully dissociated and fully associated), with the properties of the associated fluid being weighted averages of those corresponding to the self-associated and AB hypothetical fluids. Then, the enthalpy and entropy changes for the mixture, that is, ΔH^M and r^M in eq 15, are weighted averages of the enthalpy and entropy changes corresponding to two processes, namely, the formation of self-associated and complex species.

In contrast to the alcohol + inert case, it is possible that the association capability of an alcohol molecule is greater in the mixture with a proton acceptor than in the pure alcohol. A rough estimate of this capability is the ratio of oxygen atoms with respect to the total number of atoms in the molecule. Considering only carbon and oxygen atoms, this ratio is 1/5 for 1-butanol, 1/7 for 3M3P, and 2/7 for PA and BF. Hence, for the alcohol + strong proton acceptor mixtures considered here, the relative number of sites capable of forming hydrogen bonds is higher than that in the pure alcohol and, therefore, the formation of hydrogen bonds in solution may result in a decrease of the dissociation entropy upon mixing, that is, $r^M < r^P$. For the dissociation enthalpy, it is expected that $\Delta H^M < \Delta H^P$, since the association energies between the alcohol hydroxyl group and the oxygen atoms in the esters are smaller than that between two hydroxyl groups, as indicated by the quantum mechanical calculations reported in section 3.3. Stemming from the fact that $\Delta H^M < \Delta H^P$ and $r^M \neq r^P$ (most probably, $r^M < r^P$), the

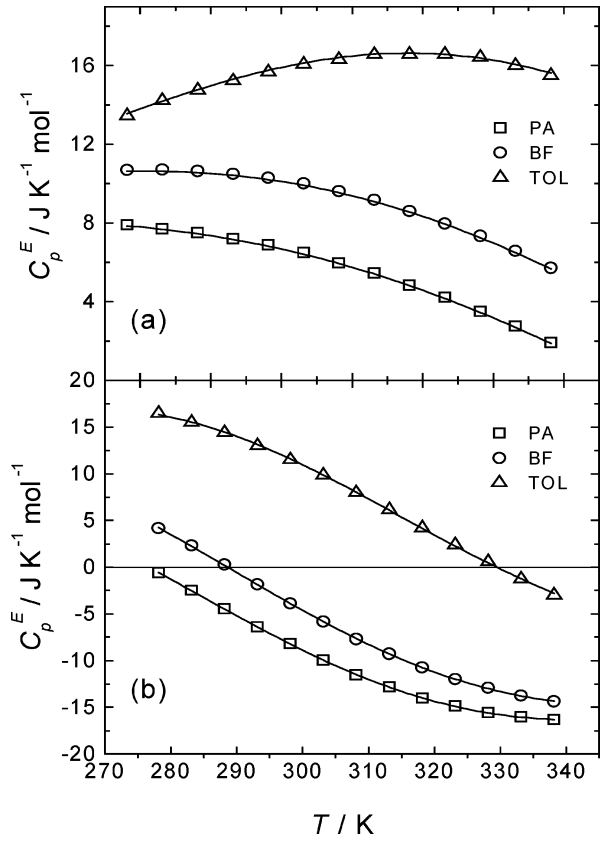

Figure 8. Equimolar excess heat capacities, C_p^E, for (a) 1-butanol + propyl acetate (PA), + butyl formate (BF), and + toluene (TOL) and for (b) 3-methyl-3-pentanol (3M3P) + propyl acetate (PA), + butyl formate (BF), and + toluene (TOL). Data for alcohol + toluene mixtures are from ref 20. Data for alcohol + ester mixtures can be found as Supporting Information. Curves are C_p^E from eq 15 using the parameter values in Table 4. Although the fittings to C_p^E were performed using data every degree, here, for clarity, data are shown every 5°.

TABLE 4: TSAM Parameters for Alcohol + Noninert Mixtures[a]

mixture	ΔH^M (J mol^{-1})	r^M	D (J K^{-1} mol^{-1})	χ^2
1-butanol + PA	16134 ± 58	37 ± 0.2	24.8 ± 0.4	0.0006
1-butanol + BF	15619 ± 24	49 ± 0.2	23.3 ± 0.4	0.0007
1-butanol + toluene	18466 ± 28	183 ± 1	15.0 ± 0.7	0.0024
3M3P + PA	14550 ± 51	147 ± 3	25.5 ± 0.9	0.0013
3M3P + BF	15146 ± 69	228 ± 6	23.1 ± 1.2	0.0032
3M3P + toluene	18903 ± 84	1081 ± 84	5.0 ± 1.7	0.0147

[a] At equimolar concentration. PA and BF stand for propyl acetate and butyl formate, respectively. The parameters were fitted using eq 15 with ΔH^P and r^P for the pure alcohols (23124 J mol^{-1} and 264.4 for 1-butanol and 19910 J mol^{-1} and 814 for 3M3P) kept as constants (see text) and $\Delta C_p = 0$. The temperature interval used in the fitting process (C_p^E every degree from eq 15) was 278.15−338.15 K. Data for mixtures containing toluene are from ref 20. 3M3P stands for 3-methyl-3-pentanol.

$C_p^E(T)$ behavior displayed in Figure 2a is expected. This is corroborated by the experimental $C_p^E(T)$ values at equimolar concentration in Figure 8 for 1-butanol and 3M3P mixed with PA and BF. Figure 8 also shows the performance of the TSAM with ΔH^M, r^M, and $(C_p^{ns})^E$ as adjustable parameters, with their values being reported in Table 4; as in the alcohol + inert case, the nonspecific contribution was $(C_p^{ns})^E = Dx_{OH}(1 - x_{OH})$, with D being a constant. For the mixtures considered, the ΔH^M values are close, with their average being 14 982 J mol^{-1}. This value is consistent with the association energy values reported in section 3.3; that is, the average value for the hydrogen bond between the alcohol and the oxygen atom of the carbonyl group and with the ester oxygen is 13 403 J mol^{-1}. Moreover, the r^M values in Table 4 are smaller than the corresponding value for the pure alcohol, r^P. This confirms that, in the presence of proton acceptor molecules, an alcohol molecule can H-bond easily. Clearly, Figure 8 shows that, despite the simplicity of the TSAM extension to mixtures and the approximations made, this model is able to describe the heat capacity behavior of alcohol + noninert mixtures well.

Figure 8 also contains $C_p^E(T)$ data[20] for equimolar mixtures of 1-butanol or 3M3P and the weak proton acceptor toluene. In this case, an a priori evaluation of the association capability is more difficult to make. On the other hand, it is expected again that $\Delta H^M < \Delta H^P$ (see section 3.3). The experimental $C_p^E(T)$ values at equimolar concentration are shown in Figure 8 together with the TSAM model curves, with the fitted ΔH^M and r^M values being shown in Table 4. The ΔH^M values are close, and their average (18 685 J mol^{-1}) is, as predicted, smaller than the ΔH values for the pure alcohols but closer to them than that in the PA and BF cases. The r^M values in Table 4 are smaller than those for the same alcohols mixed with *n*-decane (see Table 3) but much closer to the pure alcohol values than those in the PA and BF cases. Hence, it appears that, owing to its weak proton acceptor character, toluene hardly interferes with alcohol self-association.

5. Conclusions

It has been shown that the two-state association model (TSAM) is capable of describing satisfactorily the thermodynamic behavior of associated liquid systems. In particular, the TSAM gives an adequate rendering of the experimentally determined temperature and pressure dependence of the isobaric heat capacities of pure liquids. Furthermore, from the pressure dependence of C_p for pure branched alcohols, the effect of association on the volume temperature and pressure derivatives, $(\partial V/\partial T)_p$ and $-(\partial V/\partial p)_T$, was inferred. It was found that $(\partial V/\partial T)_p$ is subjected to similar, but smoother, effects than C_p, while association hardly affects $-(\partial V/\partial p)_T$. For the studied (alcohol + inert or noninert) mixtures, it appears that the $C_p^E(T)$ behavior is mainly governed by the difference between the dissociation entropy of alcohol molecules in the pure liquid and the mixture, as measured by the TSAM parameters r^P and r^M. It was found that in alcohol + inert mixtures the dissociation entropy increases upon mixing ($r^M > r^P$), while the opposite is true for alcohol + noninert mixtures ($r^M < r^P$). These results are consistent with rough estimations of the "concentration" of molecular sites capable of forming H-bonds. Moreover, the H-bond energies obtained from the TSAM compare well with those obtained from quantum mechanical ab initio calculations.

Acknowledgment. This work was supported by grants 41328Q from CONACyT-México, IN113302 from PAPIIT-UNAM, and BFM2003-09295 from the Ministerio de Ciencia y Tecnología de España. G.G.-M. and G.O.H.-S. are grateful for financial support from CONACyT-México and DGEP-UNAM.

Supporting Information Available: Tables showing (I) experimental $C_p(T,p)$ values for three pure branched alcohols—3-pentanol (3P), 3-methyl-3-pentanol (3M3P), and 3-ethyl-3-pentanol (3E3P); (II) experimental equimolar $C_p^E(T)$ values for 1-butanol + propyl acetate, 1-butanol + butyl formate, 3-meth-

yl-3-pentanol + propyl acetate, and 3-methyl-3-pentanol + butyl formate; and (III) *XYZ* coordinates for the monomers and dimers in the optimized geometries. This material is available free of charge via the Internet at http://pubs.acs.org.

References and Notes

(1) Müller, E. A.; Gubbins, K. E. *Ind. Eng. Chem. Res.* **2001**, *40*, 2193.

(2) Prausnitz, J. M.; Lichtenthaler, R. N.; Azevedo, E. G. *Molecular Thermodynamics of Fluid Phase Equilibria*, 3rd ed.; Prentice Hall PTR: Upper Saddle River, NJ, 2001.

(3) Sengers, J. V., Kayser, R. F., Peters, C. J., White, H. J., Jr., Eds. *Equations of State for Fluids and Fluid Mixtures*; Elsevier: Amsterdam, The Netherlands, and New York, 2000.

(4) Gregorowicz, J.; O'Connell, J. P.; Peters, C. J. *Fluid Phase Equilib.* **1996**, *116*, 94.

(5) Diedrichs, A.; Rarey, J.; Gmehling, J. *Fluid Phase Equilib.* **2006**, *248*, 56.

(6) Chapman, W. G.; Jackson, G.; Gubbins, K. E. *Mol. Phys.* **1988**, *65*, 1057.

(7) Lafitte, T.; Bessieres, D.; Piñeiro, M. M.; Daridon, J.-L. *J. Chem. Phys.* **2006**, *124*, 024509.

(8) Llovell, F.; Vega, L. F. *J. Phys. Chem. B* **2006**, *110*, 11427.

(9) Heintz, A. *Ber. Bunsen-Ges. Phys. Chem.* **1985**, *89*, 172.

(10) Dzida, M.; Góralski, P. *J. Chem. Thermodyn.* **2006**, *38*, 962.

(11) Piñeiro, A. *Fluid Phase Equilib.* **2004**, *216*, 245.

(12) Demirel, Y.; Paksoy, H. O. *Thermochim. Acta* **1997**, *303*, 129.

(13) Andreolli-Ball, L.; Costas, M.; Paquet, P.; Patterson, D. *Pure Appl. Chem.* **1989**, *61*, 1075.

(14) Andreolli-Ball, L.; Sun, S. J.; Trejo, L. M.; Costas, M.; Patterson, D. *Pure Appl. Chem.* **1990**, *62*, 2097.

(15) Orbey, H.; Sandler, S. I. *Fluid Phase Equilib.* **1996**, *121*, 67.

(16) Llovell, F.; Peters, C. J.; Vega, L. F. *Fluid Phase Equilib.* **2006**, *248*, 115.

(17) Cerdeiriña, C. A.; González-Salgado, D.; Romaní, L.; Delgado, M. C.; Torres, L. A.; Costas, M. *J. Chem. Phys.* **2004**, *120*, 6648.

(18) Zabransky, M.; Bures, M.; Rucicka, V. *Thermochim. Acta* **1993**, *215*, 25.

(19) Medeiros, M.; Armas-Alemán, C. O.; Costas, M.; Cerdeiriña, C. A. *Ind. Eng. Chem. Res.* **2006**, *45*, 2150.

(20) Cerdeiriña, C. A.; Tovar, C. A.; Carballo, E.; Romaní, L.; Delgado, M. C.; Torres, L. A.; Costas, M. *J. Phys. Chem. B* **2002**, *106*, 185.

(21) Paz−Ramos, C.; Cerdeiriña, C. A.; Troncoso, J.; Romaní, L. *J. Therm. Anal. Calorim.* **2006**, *83*, 263.

(22) *CDATA: Database of Thermodynamic and Transport Properties for Chemistry and Engineering* (Department of Physical Chemistry, Institute for Chemical Technology, distributed by FIZ Chemie GmbH, Berlin, Prague, 1991).

(23) Lagourette, B.; Boned, C.; Saint−Guirons, H.; Xans, P.; Zhou, H. *Meas. Sci. Technol.* **1992**, *3*, 699.

(24) Troncoso, J.; Bessières, D.; Cerdeiriña, C. A.; Carballo, E.; Romaní, L. *Fluid Phase Equilib.* **2003**, *208*, 141.

(25) Bessières, D.; Lafitte, T.; Daridon, J-L.; Randzio, S. L. *Thermochim. Acta* **2005**, *428*, 25.

(26) Gonzalez-Salgado, D.; Valencia, J. L.; Troncoso, J.; Bessieres, D.; Carballo, E.; Peleteiro, J.; Romani, L. *Rev. Sci. Instrum.*, in press, 2007.

(27) Zabransky, M.; Ruzicka, V.; Domalski, E. S. *J. Phys. Chem. Ref. Data* **2001**, *30*, 1199.

(28) Frisch, M. J.; Trucks, G. W.; Schlegel, H. B.; Gill, P. M. W.; Johnson, B. G.; Robb, M. A.; Cheeseman, J. R.; Keith, T.; Petersson, G. A.; Montgomery, J. A.; Raghavachari, K.; Al-Laham, M. A.; Zakrzewski, V. G.; Ortiz, J. V.; Foresman, J. B.; Cioslowski, J.; Stefanov, B. B.; Nanayakkara, A.; Challacombe, M.; Peng, C. Y.; Ayala, P. Y.; Chen, W.; Wong, M. W.; Andres, J. L.; Replogle, E. S.; Gomperts, R.; Martin, R. L.; Fox, D. J.; Binkley, J. S.; Defrees, D. J.; Baker, J.; Stewart, J. P.; Head-Gordon, M.; Gonzalez, C.; Pople, J. A. *Gaussian 94*, revision C.3; Gaussian, Inc.: Pittsburgh, PA, 1995.

(29) Pople, J. A.; Hariharan, P. C. *Chem. Phys. Lett.* **1972**, *66*, 217.

(30) Boys, S. F.; Bernardi, F. *Mol. Phys.* **1970**, *19*, 553.

(31) Benson, S. W. *Thermochemical Kinetics. Methods for the Estimation of Thermochemical Data and Rate Parameters*; Wiley & Sons: New York, 1976.

(32) Medeiros, M. *J. Phys. Chem. B* **2004**, *108*, 2676.

(33) Flory, P. J. *J. Am. Chem. Soc.* **1965**, *87*, 833.

(34) Costas, M.; Cáceres-Alonso, M.; Heintz, A. *Ber. Bunsen-Ges. Phys. Chem.* **1987**, *91*, 184.

(35) Unpublised data, Ourense laboratory.

(36) Cibulka, I. *Fluid Phase Equilib.* **1993**, *89*, 1.

(37) Sastry, S.; Debenedetti, P. G.; Sciortino, F.; Stanley, H. E. *Phys. Rev. E* **1996**, *53*, 6144.

(38) Gupta, R. B.; Brinkley, R. L. *AIChE J.* **1998**, *44*, 207.

(39) Desphande, D. D.; Patterson, D.; Andreoli-Ball, L.; Costas, M. *J. Chem. Soc., Faraday Trans.* **1991**, *87*, 1133.